

Implementation and Validation of LTE Downlink Schedulers for ns-3

Dizhi Zhou
Faculty of Computer Science
University of New Brunswick
Fredericton, Canada
q5frc@unb.ca

Nicola Baldo and Marco Miozzo
Centre Tecnològic de Telecomunicacions
de Catalunya
Barcelona, Spain
{nicola.baldo, marco.miozzo}@cttc.es

ABSTRACT

In LTE systems, the downlink scheduler is an essential component for efficient radio resource utilization; hence, in the context of LTE simulation, the availability of good downlink scheduler models is very important. At the time this work started, the LTE module of the ns-3 simulator only supported two types of scheduler, namely Round Robin and Proportional Fair. To overcome this limitation, we implemented in ns-3 several well-known downlink LTE scheduler algorithms, namely maximum throughput, throughput to average, blind equal throughput, token bank fair queue and priority set. In this paper, we first describe in detail their design and implementation, and then discuss their validation done by comparison with the theoretical performance in some reference scenarios.

Categories and Subject Descriptors

I.6.5 [Simulation and Modeling]: Model Development—*Modeling methodologies*; I.6.7 [Simulation and Modeling]: Simulation Support System—*Environments*

General Terms

Algorithm, Design, Performance, Verification

Keywords

Simulator, ns-3, LTE, packet scheduler, downlink

1. INTRODUCTION

Long Term Evolution (LTE) is one of the most promising standards for the fourth generation (4G) wireless networks [1]. One key component that affects the performance of an LTE system is the downlink packet scheduler in the evolved node B (eNB). Its purpose is to dynamically allocate the downlink radio resources to the user equipments (UEs) taking into consideration the varying conditions of the wireless channel, so that the quality of service (QoS) require-

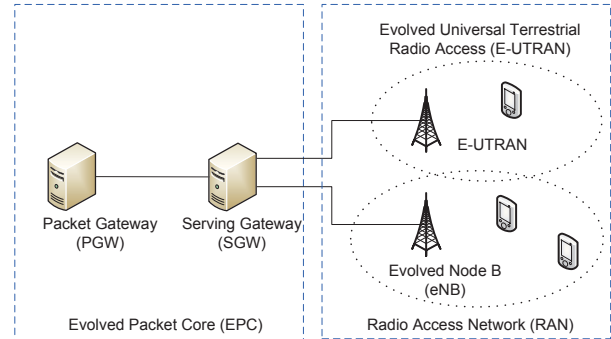


Figure 1: LTE network architecture.

ments of the UEs are satisfied. In the recent scientific literature, several downlink packet scheduling algorithms have been proposed that focus on different aspects of QoS (see for instance [2,3]), and more algorithms are expected to be investigated and proposed in the future, both by academic and industrial researchers. Because of this, in the context of the simulation of LTE systems, it is of great importance to have available a good range of well-known downlink scheduler models, so that they can not only support the end-to-end performance evaluation of LTE systems when different scheduling policies are applied, but also provide a valid reference for the development of new advanced scheduling algorithms. Unfortunately, at the time this work started, the ns-3 simulator [4] provided a very limited number of downlink scheduler models; in fact, only two types of scheduler were implemented, namely round robin (RR) and proportional fair (PF). Therefore, more scheduler models were needed so as to allow researchers to carry out more comprehensive LTE simulations with ns-3. To overcome this limitation, we implemented in ns-3 five mainstream LTE downlink scheduling algorithms mutated from the recent scientific literature, namely maximum throughput (MT) [2], throughput to average (TTA) [2], blind equal throughput (BET) [2], token bank fair queue (TBFQ) [3] and priority set (PSS) [5]. Most of these scheduling algorithms approach the radio resource allocation following either the time domain (TD) or the frequency domain (FD) approach. In the TD approach, the LTE scheduler assigns all radio resources in the current transmission time interval (TTI) to one UE. Conversely, in the FD approach, the LTE scheduler allocates the resources along both the frequency and time scales. Following this categorization, we implement both a TD and an FD version

Permission to make digital or hard copies of all or part of this work for personal or classroom use is granted without fee provided that copies are not made or distributed for profit or commercial advantage and that copies bear this notice and the full citation on the first page. To copy otherwise, to republish, to post on servers or to redistribute to lists, requires prior specific permission and/or a fee.

WNS3 2013, March 05-07

Copyright © 2013 ICST 978-1-936968-76-3

DOI 10.4108/icst.simutools.2013.251608

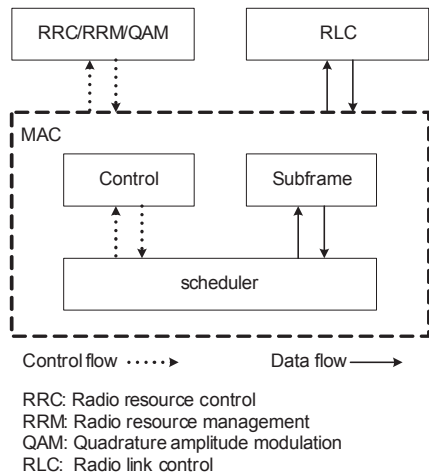


Figure 2: Structure of LTE MAC scheduler in ns-3.

for the MT, BET and TBFQ algorithms. For the TTA algorithm, which by definition follows the FD approach, we implement only the FD version. Finally, we remark that the PSS algorithm allocates the resources considering the time and frequency domains jointly, and for this reason our implementation of this algorithm does not fit into the TD/FD categorization. The source code of complete code of those schedulers can be found at [6], and has been merged in the version 3.16 of ns-3 released on December 2012.

The rest of this paper is organized as follows. We introduce the ns-3 LTE scheduler framework in section 2, and then in section 3 we describe in detail the implementation of the new downlink scheduling algorithms. In section 4 we present our approach for the validation of the scheduling algorithm implementations, which is based on the determination of their theoretical performance in some reference scenario, and its comparison with the simulation output. Finally, in section 5 we draw our conclusions.

2. FRAMEWORK

As shown in Fig. 1, the LTE model of ns-3 follows a general architecture consisting of two major parts, namely the evolved packet core (EPC) and the radio access network (RAN). The EPC is mainly responsible for mobility management, connection establishment, intra-LTE handover, and connecting the RAN to the public Internet. The RAN defines the evolved universal terrestrial radio access (E-UTRA) as the air interface that provides wireless transmission to user terminals (UEs). As common practice in cellular network, the allocation algorithm is centralized, which implies that the LTE scheduler is located in eNB. The implementation of LTE schedulers in ns-3 follows the LTE MAC scheduler interface specification [7] defined by Small Cell Forum [8]. Fig. 2 provides a sketch of such scheduler architecture. The subframe module triggers MAC scheduling at the beginning of each transmission time interval (TTI), which is the smallest unit of allocation in time of length equal to 1 ms. The LTE scheduler makes the scheduling decision based on the information provided by the control module, such as the channel quality indicator (CQI) and the radio link control (RLC) buffer status. The result of the

scheduling decision that is returned to the subframe module consists of the resource mapping between UEs and resource blocks (RB). One thing that needs to be mentioned is that, in the current LTE module of ns-3, the allocation bitmap is encoded using the allocation type 0 [9], according to which the RBs are grouped in resource block groups (RBGs). Each RBG is a set of consecutive virtual resource blocks (VRBs) of localized type as defined in section 6.2.3.1 of [10].

In what follows, we will introduce how the LTE scheduler allocates RBs to each UE, and how we implement the TD and FD schedulers. The E-UTRA is based on orthogonal frequency division multiple access (OFDMA) for the downlink and single-carrier frequency division multiple access (SC-FDMA) for the uplink. We focus on the downlink in this study. The minimum resource unit that the LTE scheduler can allocate to a UE in OFDMA is a RB, as shown in Fig. 3. Specifically, from MAC layer perspective, an RB in the time domain is one TTI and one subband in the frequency domain (180 kHz). The LTE scheduler is invoked for every TTI to allocate the resource blocks to the UEs following specific priority metrics. For the FD version, the LTE scheduler distinguishes the resources along both the frequency and time scales; hence, the minimum resource unit to allocate is a RB within a TTI. In contrast, the TD version of LTE scheduler assigns all RBs of the wideband to one UE in the current TTI. Obviously, the FD scheduler allocates radio resources in a finer granularity, but at the cost of a higher implementation complexity. The concepts just explained are valid for LTE in general; however in the ns-3 implementation, due to the constraint of using allocation type 0 only, the smallest unit of allocation is actually the RBG rather than the RB.

In the eNB, there is an Adaptive Modulation and Coding (AMC) module that assimilates the channel quality indicator (CQI) reports from UEs to estimate the wireless channel quality. In the current ns-3 model, there are two types of CQI report, namely the **wideband cqi**, which estimates the channel quality over the entire wideband, and the **subband cqi**, which is the channel quality value for a specific subband. The LTE standard does not mandate which CQI report shall be used by the scheduler to take its decision; hence, in principle the scheduler can make use of any of the CQI types. In order to study the different behavior of FD and TD schedulers, we assume that the FD version of a channel-aware scheduler exploits the **subband cqi** for the scheduling, while the corresponding TD version utilizes **wideband cqi**. As such, for the same type of LTE scheduler, the FD version has the finest control granularity for radio resource allocation but also the highest implementation complexity, whereas the TD version has the coarsest resource units but the lowest implementation complexity. The channel-unaware scheduler, such as BET, uses **wideband cqi** in both FD and TD versions.

3. IMPLEMENTATION

3.1 Maximum Throughput Scheduler

The maximum throughput (MT) scheduler [2] aims to maximize the overall throughput of an eNB. It allocates each RBG to the UE that can achieve the maximum expected data rate in the current TTI. Given N UEs, the priority metrics used in the frequency domain MT (FD-MT) and

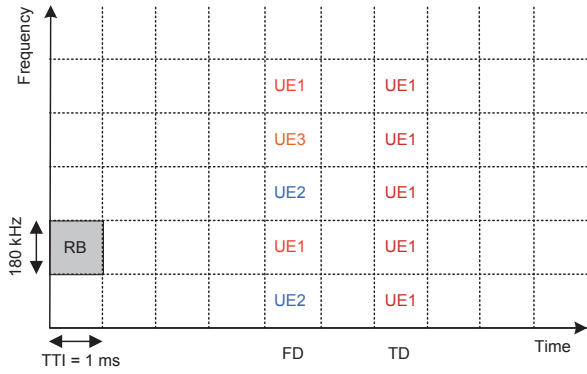


Figure 3: LTE resource allocation in the time domain and the frequency domain.

the time domain MT (TD-MT) are respectively

$$\hat{i}_k(t) = \arg \max_{j=1, \dots, N} R_j(k, t) \quad (1)$$

$$\hat{i}(t) = \arg \max_{j=1, \dots, N} R_j(t) \quad (2)$$

where $j = 1, \dots, N$ is the generic UE, $\hat{i}_k(t)$ is the UE chosen by FD-MT for transmission on the RBG k at the time interval t , and $\hat{i}(t)$ is the UE chosen by TD-MT for transmission at the time interval t over all the RBGs. Here, $R_j(k, t)$ and $R_j(t)$ are the priority metrics used for FD-MT and TD-MT, respectively; in particular, $R_j(k, t)$ is the achievable data rate for RBG k determined based on the **subband cqi** of that specific RBG, while $R_j(t)$ is the achievable data rate determined based on the **wideband cqi**. By using the above priority metrics, MT scheduler always allocates radio resources to UEs with the best channel quality. As such, the network utilization efficiency can be maximized since the network resources are always fully utilized. However, this opportunistic behavior cannot ensure fairness among UEs, which is another key performance factor.

3.2 Throughput to Average Scheduler

Different from MT, the throughput to average (TTA) scheduler [2] can be considered as the tradeoff between efficiency and fairness. The scheduling decision in TTA is performed according to the following equation:

$$\hat{i}_k(t) = \arg \max_{j=1, \dots, N} \frac{R_j(k, t)}{R_j(t)} \quad (3)$$

i.e., the priority metric of the TTA scheduler is $R_j(k, t)/R_j(t)$, which in general varies with t , j and k . From this consideration, it is evident that TTA is a FD scheduler.

3.3 Blind Equal Throughput

The blind equal throughput (BET) scheduler [2] aims to provide an equal throughput to all UEs associated with the same eNB. Unlike MT and TTA, BET is channel-unaware in the sense that both FD-BET and TD-BET use **wideband cqi** in packet scheduling. The scheduling decision for BET is performed according to the following equation:

$$\hat{i}(t) = \arg \max_{j=1, \dots, N} \frac{1}{T_j(t)} \quad (4)$$

where $T_j(t)$ is the past average throughput of UE j at time t , which is calculated by

$$T_j(t) = \beta T_j(t-1) + (1-\beta)R_j(t). \quad (5)$$

Here, β ($0 \leq \beta \leq 1$) is the weight factor for moving average, and $R_j(t)$ is the achievable data rate of UE j at time t as defined above. The TD-BET scheduler selects the UE with the largest priority metric and allocates all RBs in the current TTI to this UE. In contrast, the FD-BET scheduler first selects the UE with the lowest past average throughput (largest priority metric) and assigns one RBG to this UE. Then, the scheduler recalculates its expected throughput and continues to allocate more RBG blocks to this UE if the updated past average throughput is still no greater than other UEs. This procedure continues until the expected throughput of this UE is no longer the lowest. The scheduler assigns RBG blocks to other UEs in the same way until all RBGs are allocated. The rationale behind this algorithm is to ensure an equal throughput among all UEs in every TTI.

3.4 Token Bank Fair Queue Scheduler

The Token bank fair queue (TBFQ) [3] is a QoS aware scheduler which derives from the leaky-bucket mechanism. In TBFQ, the traffic flow of a generic UE $i = 1, \dots, N$ is characterized by following parameters:

- t_i : packet arrival rate;
- r_i : token generation rate;
- p_i : token pool size;
- E_i : counter that records the number of token borrowed from or given to the token bank by flow i ; E_i can be smaller than zero;

Each k bytes data consumes k tokens. Also, TBFQ maintains a shared token bank (B) so as to balance the traffic between different flows. If token generation rate r_i is bigger than packet arrival rate t_i , then tokens overflowing from token pool are added to the token bank, and E_i is increased by the same amount. Otherwise, flow i needs to withdraw tokens from token bank based on a priority metric $\frac{E_i}{r_i}$, and then E_i is decreased. Obviously, the UE that contributes more to the token bank has a higher priority to borrow tokens; on the other hand, the UE that borrows more tokens from the bank has a lower priority to continue to withdraw tokens. Therefore, in case of several UEs having the same token generation rate, traffic rate and token pool size, UE suffering from higher interference has more opportunity to borrow tokens from bank. In addition, TBFQ can police the traffic by setting the token generation rate to limit the throughput. Besides, TBFQ maintains following three parameters for each flow:

- d_i : debt limit; if E_i belows this threshold, UE i cannot further borrow tokens from bank. This is for preventing an UE to borrow too much tokens.
- c_i : the maximum number of tokens UE i can borrow from the bank each time.
- C : once E_i reaches the debt limit d_i , the UE i must store C tokens to the bank in order to borrow further tokens.

We implement two versions of the TBFQ scheduler: frequency domain TBFQ (FD-TBFQ) and time domain TBFQ (TD-TBFQ). In FD-TBFQ, the scheduler always selects the UE with the highest metric and allocates RBG with the highest `subband cqi` until there are no packets in the UE's RLC buffer or all RBGs are allocated [11]. In TD-TBFQ, after selecting the UE with maximum metric, all the RBGs are allocated to this UE by using the `wideband cqi` [3]. In the current implementation, the token generation rate is configured according to the guarantee bit rate (GBR) specified by the EPS bearer QoS parameters.

3.5 Priority Set Scheduler

The Priority set scheduler (PSS) is another QoS aware scheduler which combines time domain (TD) and frequency domain (FD) packet scheduling operations into one scheduler [5]. It controls the fairness among UEs by defining a specified target bit rate (TBR). In the TD part of the scheduler, PSS first selects those UEs with a non-empty RLC buffer, and then divides them into two sets based on the TBR:

- set 1: UEs whose past average throughput is smaller than TBR; TD scheduler calculates its priority metric $p_k^1(t)$ following the blind equal throughput (BET) approach:

$$p_k^1(t) = \frac{1}{T_j(t)} \quad (6)$$

- set 2: UEs whose past average throughput is larger (or equal) than TBR; TD scheduler calculates its priority metric $p_k^2(t)$ following the proportional fair (PF) approach:

$$p_k^2(t) = \frac{R_j(k, t)}{T_j(t)} \quad (7)$$

Here, $R_j(k, t)$ is the achievable data rate for UE j at time t on the k -th RBG and $T_j(t)$ is the past average throughput of UE j at time t . The UEs belonging to set 1 are considered with a higher priority than those in set 2. PSS selects N_{mux} UEs with the highest metric in the two sets and forward those UEs to FD scheduler. In PSS, FD scheduler allocates a RBG to the UE with largest metric. On this matter, two algorithms have been considered in this work:

- Proportional fair scheduled (PFsch)

$$M\hat{s}ch_k(t) = \max_{j=1, \dots, N} \frac{R_j(k, t)}{Tsch_j(t)} \quad (8)$$

- Carrier over interference to average (CoIta)

$$M\hat{c}oi_k(t) = \max_{j=1, \dots, N} \frac{CoI[j, k]}{\sum_{k=0}^{N_{RBG}} CoI[j, k]} \quad (9)$$

where $Tsch_j(t)$ is similar to the past average throughput of UE j , with the difference that it is updated only when the UE is actually served. $CoI[j, k]$ is an estimation of the signal to interference plus noise ratio (SINR) on the RBG k of UE j . Both PFsch and CoIta is for decoupling FD metric from TD scheduler. In addition, FD scheduler also provides a weight metric $W[n]$ for helping controlling fairness in the case of a low number of UEs.

$$W[n] = \max(1, \frac{TBR}{T_j(t)}) \quad (10)$$

Table 1: System parameters common to all experiments.

Parameter	Value
Number of RBs	25
RBs per RBG	2
AMC model	PiroEW2010 [12]
Error model of control	Deactivated
Error model of data	Deactivated
Path loss model	Friis spectrum propagation
Mobility model	Constant position
Transmission power	eNB: 30 dBm; UE: 23 dBm
Noise figure	eNB: 5 dB; UE: 5 dB
TTI	1 ms
Number of UEs (N)	$N \leq 5$
UE and eNB distance	0, 3, 6, 9, 12, 15 km
Simulation time	1 second

Therefore, on RBG k , the FD scheduler selects the UE j that maximizes the product of the frequency domain metric by weight $W[n]$. This strategy will guarantee the throughput of lower quality UEs tending toward their TBR. In the implementation, the target bit rate of PSS has been implemented as the maximum bit rate (MBR) in EPC bearer QoS parameters of the LTE MAC scheduler interface specification [7].

4. VALIDATION

We now validate the scheduler implementations described in the previous section by comparing their simulation performance with the theoretical performance in some reference scenarios. The decision of validating against theoretical performance is mainly motivated by the lack of equivalent measurements from real LTE deployments to could be used for the same purpose. We chose a set of scenarios with specific simplifying assumptions so that it was feasible to determine the theoretical performance of the scheduling algorithms, and verify the correctness of the scheduler implementations. We note that, due to these simplifying assumptions, these scenarios are not necessarily representative of real deployments; in fact, large scale simulation campaigns involving realistic scenarios are beyond the scope of this paper, and are therefore left for future study. For each chosen scenario, we calculate the reference throughput for each UE, and check that the obtained throughput matches the reference throughput within a given tolerance (equal to 10% of the throughput in this paper). The complete test suites can be found in [6].

The values of the simulation parameters that are common to all the considered scenarios are given in Table 1. As fading is not considered and the UEs are configured as stationary nodes, each UE will have the same SINR during the whole simulation. In other words, both `wideband cqi` and `subband cqi` of UEs are constants and their values are only related

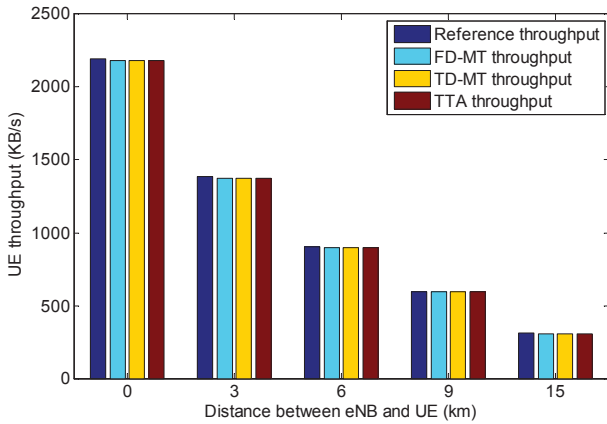


Figure 4: UE throughput in FD-MT, TD-MT and TTA schedulers (scenario I and II, $N = 3$).

to the distance between UE and eNB. We stress that, since the allocation bitmap is coded in allocation type 0, the minimum unit of allocation is resource block group (RBG), which contains two RBs in all the test cases here [13].

In addition, we use different traffic patterns for QoS aware and QoS unaware schedulers. Specifically, in MT, TTA and BET, which are QoS unaware schedulers, we assume that the RLC buffer for each UE is always saturated by using the ns-3 RLC saturation mode (RLC/SM) model. In this way, the simulation can fully reflect the RBG allocation behavior of different scheduling algorithms. On the other hand, for TBFQ and PSS, UDP traffics with different constant bit rates are generated so as to validate the unique feature of those QoS aware schedulers.

For all schedulers in this paper, we test two basic scenarios:

- scenario I: all UEs have the same distance to the eNB, so that all UEs have the same **wideband cqi** and **subband cqi**;
- scenario II: each UE has a different distance to the eNB, so that each UE has the different **wideband cqi** and **subband cqi**;

The simulation time for all test cases is 1 seconds so as to decrease the total testing time in ns-3. This choice is acceptable due to the stationarity of the CQI throughout the simulation, which results in a very short convergence time of the performance of the scheduling algorithms. In this section, we use T_X^Y to represent the reference throughput of UE for scheduler X in scenario Y . The number of UEs is denoted as N which is shown in the end of each figure. We would like to stress that the validation is focused on throughput statistics since all of the algorithms have policies based on the assigned resources in terms of bitrate and this work aims at verifying their correct design. We left for future for future work a more in depth analysis with more realistic scenarios and other statistics (e.g., delay, jitter, fairness, etc.).

4.1 MT and TTA

Since according to the scenario configuration both the **wideband cqi** and the **subband cqi** of UEs are constant, the achievable data rate selected by adaptive modulation

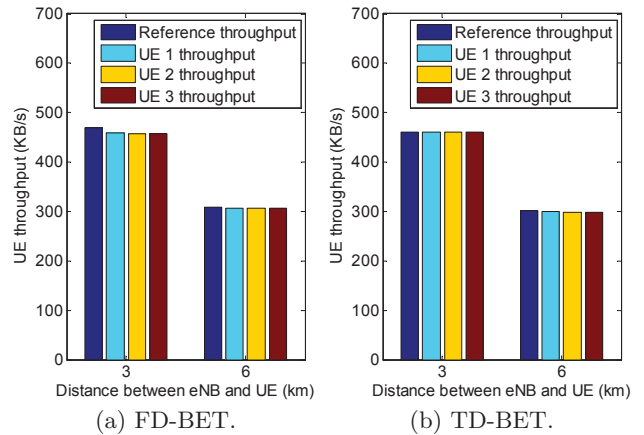


Figure 5: UE throughput of FD-BET and TD-BET schedulers (scenario I, $N = 3$).

and coding (AMC) is also the constant during the simulation. Therefore, for FD-MT, TD-MT and TTA in scenario I, all UEs have the same priority metrics. In this case, the current implementation always allocates all RBGs to the first UE connected to eNB, which is the first UE defined in the script since UEs are served in a FIFO order. In addition, because **wideband cqi** and **subband cqi** are only related to the distance between UE and eNB (there is no interference from other cells), the UE closer to eNB has the higher achievable data rate in both wideband and subband. Therefore, for FD-MT, TD-MT and TTA in scenario II, the schedulers will always allocate all RBs to the UE closest to eNB. In summary, in MT and TTA, the reference throughput T in both scenario I and II is

$$T_{fdmt,tdmt,tta}^{I,II} = \frac{S(MCS, B)}{\tau} \quad (11)$$

Here τ is the TTI duration; B is the total number of RBs which can be used (24 throughout this paper, because of the transmission bandwidth configuration and the RBG size); MCS is the modulation and coding scheme in use at the given SINR; finally, $S(MCS, B)$ is the transport block size as defined in [13]. According to the scheduler behavior in the scenario considered, $T_{fdmt,tdmt,tta}^{I,II}$ represents the achievable data rate of the UE receiving all the resources, while the reference throughputs of other UEs are zero. Fig. 4 shows the simulation results for FD-MT, TD-MT and TTA in scenario I by different distance between UE and eNB. The right three columns represent the throughput of the first UE defined in script by using different schedulers. The throughputs of the other UEs are zero and are not shown in the figure. We can see that the simulated throughput matches reference throughput very well which is shown in the left column.

4.2 BET

The expected behavior in the long term of both TD-BET and FD-BET in scenario I and II is a fair division of the resources among the UEs, independently from their position and/or channel conditions. However, the reference throughputs of UEs in scenario I and scenario II are different.

In scenario I, all UEs can obtain the same achievable data rate due to the identical **wideband cqi**. Then the behavior of FD-BET in this case is that it allocates each RBG to

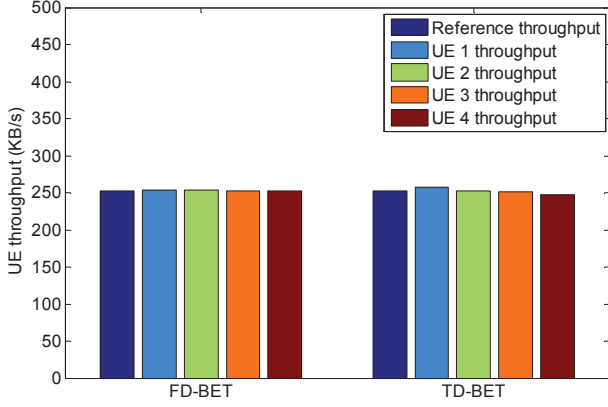


Figure 6: UE throughput of FD-BET and TD-BET schedulers (scenario II, $N = 4$).

each UE in turn until all RBs are allocated to UEs. On the other hand, TD-BET works as the round robin scheduler that it allocates all RBGs to a UE in current TTI and assigns all RBGs to another UE in next TTI. If we assume that the number of RBGs is an integer multiple of N , then we have the following equations for reference throughputs of FD-BET and TD-BET:

$$T_{fdbet}^I = \frac{S(MCS, \frac{B}{N})}{\tau} \quad (12)$$

$$T_{tdbet}^I = \frac{S(MCS, B)}{\tau \times N} \quad (13)$$

FD-BET allocates $\frac{B}{N}$ RBs to each UE per TTI while TD-BET allocates B RBGs in every N TTIs. The simulation results of FD-BET and TD-BET in scenario I can be found in Fig. 5. In Fig. 5, we can see that all UEs have the same throughputs which match the reference throughput very well.

In scenario II, four UEs are placed at different distance to eNB so that the AMC will assign different achievable data rate to each UE according to its respective **wideband cqi**. In this case, FD-BET will allocate a different number of RBGs to each UE. Besides, the time slot between two scheduling events for one UE in TD-BET is also variable. Therefore, we cannot use the same reference throughput equations of scenario I in this case. Let us consider first TD-BET in scenario II. Let F_i be the fraction of time allocated to UE i in total simulation time, R_i^{fb} be the full bandwidth achievable data rate for UE i , and T_i be the achieved throughput of UE i . Then we have:

$$T_i = F_i \times R_i^{fb} \quad (14)$$

In TD-BET, the sum of F_i for all UEs equals one. Then we can rearrange Eq. (14) to

$$\sum_i \frac{T_i}{R_i^{fb}} = 1 \quad (15)$$

In long term, all UEs have the same T_i so that we replace T_i by T . Then the reference throughput of TD-BET in scenario II is:

$$T_{tdbet}^{II} = \frac{1}{\sum_{i=1}^N \frac{1}{R_i^{fb}}} \quad (16)$$

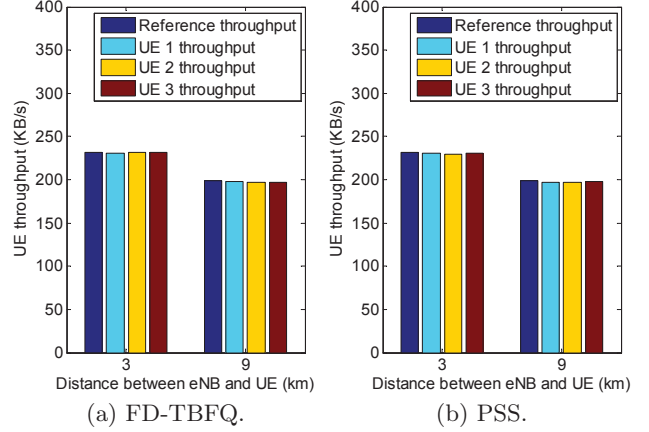


Figure 7: UE throughput of FD-TBFQ and PSS schedulers (scenario I, $N = 3$).

Eq. (16) can also be used to calculate reference throughput for FD-BET in scenario II. In our testings, each UE obtains the same total amount of RBGs in both FD-BET and TD-BET. In addition, by the transport block size table in [13], we know that $\sum_i S(MCS, B_i)$ approximately equals to $S(MCS, B)$, where $B = \sum_i B_i$. Here, B_i is the number of RBs allocated to UE i in FD-BET for one TTI. In other words, it means that if the UE can obtain the same number of RBGs, the long term throughput of UE in both FD-BET and TD-BET will be very close to each other. Therefore, we can also use the Eq. (16) to calculate T_{fdbet}^{II} . The simulation results of FD-BET and TD-BET in scenario II can be found in Fig. 6, which shows the case of four UEs placed at distance of 0, 3, 6 and 9 kilometers (km) to eNB. It is clear that the obtained throughput matches the reference throughput very well.

4.3 TBFQ and PSS

TBFQ and PSS are two QoS aware schedulers. In order to test their QoS features, we simulate UDP flows with various constant bit rates. In addition, the packet sending interval is set to 1 ms to keep the RLC buffer non-empty. Since the **wideband cqi** and **subband cqi** are constant, FD-TBFQ and TD-TBFQ will perform exactly the same. Therefore, in the rest of this section, we only discuss how to validate the FD-TBFQ scheduler. In each simulation, we use the same UDP traffic rate and radio bearer specification among UEs. For each UE, the token generation rate in FD-TBFQ and the target bit rate in PSS are configured to the corresponding UDP traffic rate. For PSS, we select PFsch as the FD scheduler; the same testing results can also be obtained by using ColtA in the FD scheduler. The TD scheduler of PSS will always select and forward half of the total UEs to the FD scheduler.

In scenario I, because each flow has the same traffic rate t_i and token generation rate r_i , FD-TBFQ scheduler will guarantee the same throughput among UEs. In addition, the exact reference throughput of UE is depended on the total UDP traffic rate:

$$T_{fdbtbfq}^I = t_i, \text{ if } \sum_i t_i < T_t \quad (17)$$

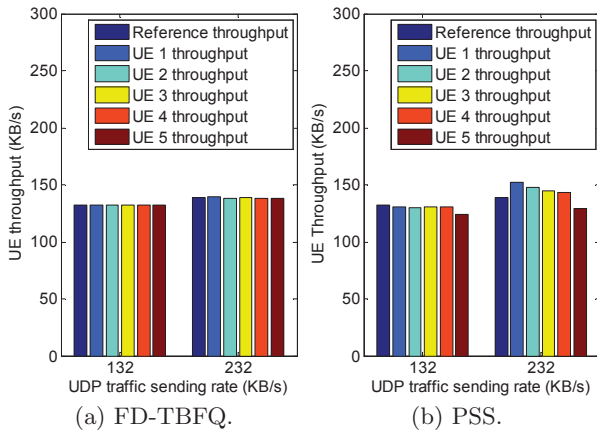


Figure 8: UE throughput of FD-TBFQ and PSS schedulers (scenario II, $N = 5$).

$$T_{fdtbfq}^I = \frac{T_t}{N}, \text{ if } \sum_i t_i \geq T_t \quad (18)$$

where $T_t = \frac{S(MCS,B)}{\tau}$. Here, T_t is the maximum total throughput which equals to the achievable data rate $\frac{S(MCS,B)}{\tau}$ when all RBGs are allocated to one UE. When the total traffic rate ($\sum_i t_i$) is smaller than maximum total throughput T_t , FD-TBFQ can police the traffic by token generation rate r_i so that the reference throughput of UE equals its traffic rate (as the token generation rate is set to the traffic generation rate in this study). On the other hand, when total traffic rate is bigger than the maximum total throughput T_t , the eNB cannot serve all the UEs in one TTI. Therefore, in each TTI, FD-TBFQ will allocate all RBGs to one UE due to the large RLC buffer size. When that UE is scheduled in current TTI, its token counter E_i is decreased so that it will not be scheduled in the next TTI. Because each UE has the same traffic generation rate t_i , FD-TBFQ will serve each UE in turn and only serve one UE per TTI. Therefore, the reference throughput of an UE in the second condition equals to an even share of the maximum total throughput.

For the PSS scheduler in scenario I, since all UEs have the same achievable data rate, the PSS will perform like BET because both metrics in the FD and TD scheduler are determined by past average throughput. Therefore, PSS and FD-TBFQ have the same maximum total throughput. We can use the same method in Eq. (17) and Eq. (18) to calculate the reference throughput T_{pss}^I . The simulation results of FD-TBFQ and PSS in scenario I can be found in Fig. 7. In Fig. 7, we can clearly see that the UE throughput of the UE at a 9 km distance case is smaller than the traffic rate (232 KB/s). This is because that the total UDP traffic rate is bigger than the maximum total throughput. In addition, for the UE at a 3 km distance, the obtained throughput equals the traffic rate. This is because the UE throughput is limited by token generation rate in FD-TBFQ and by the target bit rate in PSS.

Also in scenario II the reference throughputs of UEs in FD-TBFQ and PSS depend on the maximum total throughput T_t . However, the maximum total throughput in this case has a different value compared to scenario I. Similar to the case of scenario I, FD-TBFQ and PSS perform like

the BET scheduler when the total traffic rate is bigger than the maximum total throughput. Therefore, in scenario II, T_{fdtbfq}^{II} and T_{pss}^{II} can be calculated using the same method in Eq. (17) and Eq. (18), but considering a different formulation of $T_t = \frac{N}{\sum_{i=1}^N \frac{1}{R_i^{fb}}}$. The simulation results of FD-TBFQ

and PSS in scenario II are shown in Fig. 8; in this case, the UEs are placed respectively at a distance of 0, 3, 6, 9 and 15 kilometers from the eNB. The UE throughput variance in PSS is bigger than that in FD-TBFQ, but it is still within the chosen tolerance setting. This variance is due to the slower convergence time of the PSS scheduler, and it largely decreases when longer simulations are conducted.

5. CONCLUSION

In this paper we described the implementation of several LTE downlink scheduling algorithms for ns-3, namely maximum throughput (MT), throughput to average (TTA), blind equal throughput (BET), token bank fair queue (TBFQ) and priority set (PSS), and we presented our validation study that compared the simulation output produced by the implemented schedulers with the theoretical performance in some reference scenarios. As shown by our results, our validation study guarantees within an acceptable tolerance the correct operation of our new scheduler implementations.

As future work, we plan to analyze more in depth the performance of the schedulers by means of simulation, considering realistic scenarios and more statistics.

6. ACKNOWLEDGMENTS

This work has been partially funded by the Google Summer of Code 2012 program. The work at the University of New Brunswick has also been partially funded by a research grant from the Natural Sciences and Engineering Research Council (NSERC) of Canada. The work at CTTC has also been partially funded by the Spanish Ministry of Science and Innovation under grant number TEC2011-29700-C02-01 (project SYMBIOSIS), and by the Catalan Regional Government under grant 2009SGR-940.

The authors would like to thank L. Suresh, T. Henderson and B. Bojovic for their constructive and insightful comments.

7. REFERENCES

- [1] A. Ghosh, R. Ratasuk, B. Mondal, N. Mangalvedhe, and T. Thomas. LTE-Advanced: Next-generation wireless broadband technology. *ACM Transactions on Multimedia Computing, Communications, and Applications*, 17(3):10–22, Jun. 2010.
- [2] F. Capozzi, G. Piro, L. A. Grieco, G. Boggia, and P. Camarda. Downlink packet scheduling in LTE cellular networks: Key design issues and a survey. *IEEE Communications Surveys & Tutorials*, 99(1-23), Jun. 2012.
- [3] W.K. Wong, H.Y. Tang, and V.C.M. Leung. Token bank fair queuing: a new scheduling algorithm for wireless multimedia services. *ACM Int. J. Commun. Syst.*, 17(6):519–614, Aug. 2004.
- [4] The network simulator - ns-3. <http://www.nsnam.org/>.
- [5] G. Mongha, K.I. Pedersen, I.Z. Kovacs, and P.E. Mogensen. Qos oriented time and frequency domain

- packet schedulers for the utran long term evolution. In *Proc. IEEE VTC Spring*, May 2008.
- [6] Ns-3 lte scheduler repository.
<http://code.nsnam.org/dizhizhou/ns-3-dev>.
 - [7] Femto Forum. LTE MAC scheduler interface specification, Dec. 2010.
 - [8] Small cell forum. <http://www.smallcellforum.org/>.
 - [9] 3GPP. E-UTRA user equipment (ue) radio transmission and reception. 3GPP TS 36.101, Sep. 2012.
 - [10] 3GPP. E-UTRA physical channels and modulation. 3GPP TS 36.211, Dec. 2011.
 - [11] F.A. Bokhari, H. Yanikomeroglu, W.K. Wong, and M. Rahman. Cross-layer resource scheduling for video traffic in the downlink of ofdma-based wireless 4g networks. *EURASIP J. Wirel. Commun. Netw.*, 2009(3), Jan. 2009.
 - [12] G. Piro, L.A. Grieco, G. Boggia, and P. Camarda. A two-level scheduling algorithm for qos support in the downlink of lte cellular networks. In *European Wireless Conference*, Apr. 2010.
 - [13] 3GPP. E-UTRA physical layer procedures. 3GPP TS 36.213, Mar. 2012.